Submitted to the 30th International Conference on High-Energy Physics ICHEP2000,
Osaka, Japan, July 2000

Measurement of the Photoproduction Cross Section with a Leading Proton at HERA

H1 Collaboration

Abstract

The total cross-section for the semi-inclusive photoproduction process with a leading proton in the final state has been measured at centre-of-mass energies between 91 and 231 GeV. The measured cross-sections refer to the kinematic range with transverse momenta of the scattered proton restricted to $p_T \leq 0.2$ GeV and $0.66 \leq z \leq 0.90$, where $z = E'_p/E_p$ is the scattered proton energy normalized to the beam energy. That is a region, in which diffractive processes are suppressed relative to processes with pion and reggeon exchange. The cross-section is measured to be about $7.7\,\mu$b per unit z. It is found to be independent of the photon-proton centre-of-mass energy and the scattered proton momentum. The measured cross-sections are compared with semi-inclusive deep inelastic scattering data with a leading proton in the final state, which is subject to the same kinematic restrictions as in the case of photoproduction. This allows to study the transition from finite photon virtuality Q^2 to $Q^2 = 0$ in a model in which the proton structure function at low Q^2 is split into a nonperturbative vector meson dominated contribution and a partonic contribution. The VDM contribution determined in the framework of this model in case of the semi-inclusive process is only 23% of the amount found in the inclusive reaction.

Abstract: 967
Parallel session: PA-02
Plenary talk: PL-12

1 Introduction

The HERA electron proton collider allows to reconsider an old problem in deep inelastic lepton scattering (DIS) concerning the transition of photoproduction with virtual photons of virtuality Q^2 to photoproduction with real photons at $Q^2 = 0$. Only now sufficient data become available at the same centre-of-mass energy for both reactions, which are recorded within the same experimental set-up so that the bulk of systematic errors are identical and will have no impact on the analysis. Such type of investigations have been performed by the HERA experiment H1 [1] for inclusive DIS and photoproduction final states. The present paper deals with the transition in semi-inclusive reactions with a forward scattered proton in the final state.

The transition from finite Q^2 reactions to the limiting case of $Q^2 = 0$ is conveniently described by introducing a total virtual photon proton cross-section[1]

$$\sigma^{tot}_{\gamma^{(*)}p}(W, Q^2) \approx \frac{4\pi^2\alpha}{Q^2} F_2(x, Q^2) \tag{1}$$

where $x = Q^2/(2p \cdot q)$ is the Bjorken scaling variable with p and q being the four-momenta of the incident proton and photon respectively. α is the fine-structure constant and F_2 the proton structure function. W denotes the total $\gamma^* p$ centre-of-mass energy, which for the present application of small values of the scaling variable x can be approximated by $W^2 \approx Q^2/x$.

The transition $Q^2 \to 0$ has to obey boundary conditions imposed by conservation laws and by measurements. Due to the conservation of the electromagnetic current, F_2 has to vanish as Q^2 tends to 0. The other boundary condition which has to be obeyed is based on an experimental observation. Measurements in DIS reactions show that the total $\gamma^* p$ cross-section at low x follows a power law behaviour [1]

$$\sigma^{tot}_{\gamma^{(*)}p} \propto (W^2)^\lambda.$$

The values of the parameter λ increase with increasing Q^2 and range between 0.15 at $Q^2 = 0.9\,\text{GeV}^2$ and 0.2 at $Q^2 = 3\,\text{GeV}^2$. In the case of photoproduction λ approaches the so called soft pomeron limit of 0.08 [2].

It is interesting to compare this transition for inclusive processes with semi-inclusive DIS processes where the proton remains intact leaving the interaction with a fractional energy[2] $z = E'_p/E_p$, where E'_p and E_p are the energies of the incident and scattered protons respectively. The process is sketched in Figure 1. In a previous publication [3] it has been demonstrated that in the kinematic range of this experiment $0.66 \le z \le 0.90$ the semi-inclusive reaction is dominated by processes where the virtual photon interacts with colorless constituents of the proton. In Regge terminology, this corresponds to a hadronic exchange object $\mathcal{R}$, a reggeon or a virtual pion in the kinematic range of z under study, colliding with the photon at fixed energy $(1-z)E'_p$. The variables describing this process are $\beta = x/(1-z)$ instead of x and the invariant mass of the $\gamma\mathcal{R}$ system $M_X = W\sqrt{1-z}$. Note that for each value of z, the choice of W fixes M_X.

[1]The exact formula used is $\sigma^{tot}_{\gamma^* p}(W, Q^2) = (\frac{4\pi^2\alpha}{Q^4})(4M_p^2 x_p^2 + Q^2)/(1-x) \cdot F_2(x, Q^2)$, M_p being the proton mass.

[2]In some publications, $x_{I\!P} = 1 - z$ is used instead.

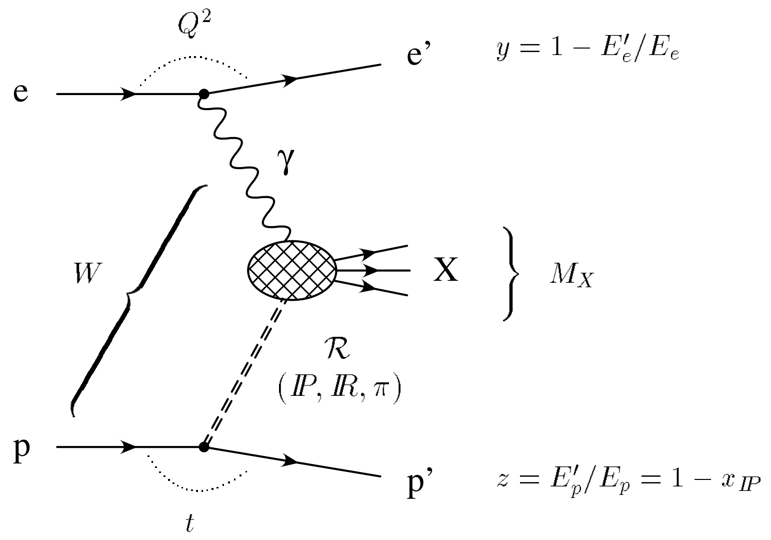

Figure 1: *The process $ep \to e'p'X$. At the proton vertex, $z = E'_p/E_p$ is the fractional momentum kept by the proton.*

A comparison of semi-inclusive data with a leading proton in the final state at finite values of Q^2 with data at $Q^2 = 0$ thus investigates the limit $Q^2 \to 0$ for $\gamma I\!R$ or $\gamma\pi$ reactions. In order to avoid uncertainties due to flux factors describing the probability to hit $\mathcal{R}$ ($\mathcal{R} = I\!R, \pi$) in a proton, the measurement need not be converted into a $\gamma I\!R$ or $\gamma\pi$ cross section. Instead the flux factors can be considered as a common normalisation parameter for photoproduction and DIS.

In the present paper measurements of the semi-inclusive photoproduction process $\gamma p \to p'X$ will be described, which are then combined with the corresponding DIS data from the same experiment published in [3], where the proton is subject to the same kinematic restrictions in both cases.

2 Apparatus

The H1 detector is described in detail elsewhere [4]. In this paper we make use of the H1 coordinate system, originating at the nominal interaction point. It is defined as follows: the direction of the incoming proton beam is taken as the $+z$ axis, the x axis points towards the centre of the storage rings, and the y axis points upwards w.r.t. the plane of the HERA electron ring.

The main H1 components used for this analysis are:

- The **central tracking chambres** CJC1 and CJC2 and the **central proportional chambres** CIP and COP for trigger purposes. They are of cylindrical shape, enclosing the beam pipe along the beam line. Charged particle momenta are calculated from the curvature introduced by the 1.2 Tesla field of the H1 solenoid. The momentum resolution is $\sigma_p/p^2 \approx 10^{-2}\,\mathrm{GeV}^{-2}$ at momenta relevant for this analysis. The track triggers are efficient for tracks with a transverse momentum $p_T^{\mathrm{trk}} > 450\,\mathrm{MeV}$.

- The **luminosity system**, consisting of electron calorimeters and a photon detector, is located downstream of the H1 detector. It is capable of measuring the luminosity online with a precision of better than 1% by selecting events for the Bethe-Heitler process $ep \rightarrow e'p'\gamma$.

  In 1996, two electron calorimeters, ETAG33 and ETAG44, were operated at $z = -33$ m and $z = -44$ m from the nominal H1 interaction point. The system is used to identify photoproduction events where a quasi-real photon is emitted by the incident lepton and the scattered lepton being observed in one of the small angle electron calorimeters. Due to the acceptance of the electron detectors, the virtuality of the photon is restricted to $Q^2 < 0.01\,\text{GeV}^2$ for tagged photoproduction events.

- The **Forward Proton Spectrometer (FPS)** [5] is used to measure the trajectory of protons which are scattered under small angles at the interaction point. In 1996, two stations were operated at distances of 81 m and 90 m from the H1 interaction region. The FPS stations consist of detectors housed in movable plunger vessels, so called Roman Pots, which are moved into the HERA machine vacuum when stable beam conditions are established. A track measurement is performed by four fiber hodoscopes per station. The hodoscopes are sandwiched between scintillator planes for triggering purposes.

  Scattered proton momenta are reconstructed from the deviation of their trajectories at the position of the Roman Pots from the actual stored beam orbit. Thus in a calibration procedure, the position of the circulating beam with respect to the nominal beam is determined for each proton fill. The track segments of each station are combined into a local vector tangential to a proton trajectory at 85 m from the collision point. Making use of the known properties of the HERA beam optics, the scattering angle at the interaction point and the energy of the scattered proton can be inferred from the parameters of the measured local trajectory vector. This procedure results in an error on the energy measurement of less than $8\,\text{GeV}$. The detector size, the distance of the detector stations from the interaction point, and the proton beam size restrict the acceptance in the proton's transverse momentum to $p_T \leq 0.2\,\text{GeV}$ and in the two projections x and y to values below $|\theta_x|, |\theta_y| < 0.5\,\text{mrad}$. Proton energies $500\,\text{GeV} \leq E'_p \leq 780\,\text{GeV}$ are accepted by the spectrometer. For the present analysis the energy range was further restricted to $0.66 \leq z = E'_p/E_p \leq 0.90$.

3 Data Selection

The analysis is based on a data set from the 1996 running period, where HERA collided $820\,\text{GeV}$ protons with $27.5\,\text{GeV}$ positrons. Data were analysed where the FPS was in a stable position close to the circulating beam and all relevant components of the H1 detector were fully operational. The corresponding integrated luminosity amounts to $3.3\,\text{pb}^{-1}$.

In order to study the reaction $\gamma p \rightarrow p'X$, events were selected with a reconstructed track through both FPS stations at $z = 81$ m and $z = 90$ m, a positron candidate in one of the small-angle electron detectors and at least one reconstructed track with $p_T^{\text{trk}} > 500\,\text{MeV}$ in the central H1 detector.

The distributions of emission angle projections as a function of the energy of the scattered proton are shown in Figure 2.

For the analysis, the data are grouped into five $40\,\mathrm{GeV}$ wide bins in the energy range $540\,\mathrm{GeV} \leq E'_p \leq 740\,\mathrm{GeV}$. The measured cross-sections correspond to an integral over $p_T < 200\,\mathrm{MeV}$ in the scattered proton's transverse momentum. In order to be accepted for the analysis, the kinematic quantities of the scattered proton were required to lie within a fiducial volume defined as limits on the projected angles as a function of the proton's energy. This results in maximum values for the scattering angles of $|\theta_x|, |\theta_y| < 0.3\,\mathrm{mrad}$.

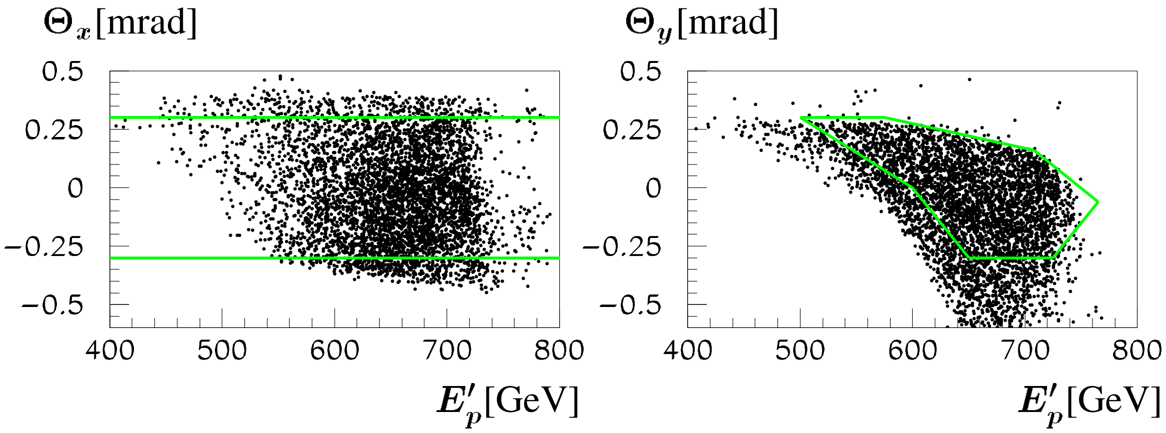

Figure 2: *The projection of the proton's polar scattering angle onto the x and y axis in dependence on the proton's energy for the selected data sample. The borders of the fiducial volume explained in the text are indicated.*

The positron candidates in ETAG33/ETAG44 were accepted if there was an energy deposition between $8.3\,\mathrm{GeV}$ and $19.3\,\mathrm{GeV}$ in ETAG33 or larger than $20\,\mathrm{GeV}$ in ETAG44 and if a cut on the energy deposition in the photon detector rejecting Bethe-Heitler overlay events was fulfilled. The data sample was binned according to the value of the inelasticy $y = 1 - E'_e/E_e$, where E'_e is equal to the energy measured in the tagger calorimeters and E_e is the positron beam energy. The ETAG33 acceptance varies for the considered y range of $0.3 \leq y \leq 0.7$ between 8% and 66%. ETAG44 accepts events within $0.04 \leq y \leq 0.2$. A mean acceptance of 29% was determined for events with an energy deposition in ETAG44. All events of the ETAG44 sample form one bin. The ETAG33 sample resulted in two bins. The values for the mean γp centre-of-mass energy W, calculated as $W = \sqrt{ys}$, for the three bins are: $W_{ETAG44} = 91\,\mathrm{GeV}$, $W_{ETAG33,1} = 187\,\mathrm{GeV}$, $W_{ETAG33,2} = 231\,\mathrm{GeV}$.

At least one track in the H1 detector was required to have a transverse momentum of $p_T^{\mathrm{trk}} > 500\,\mathrm{MeV}$, and a polar angle θ of $20^\circ < \theta < 160^\circ$ in order to guarantee a reasonable trigger efficiency. The correction due to this cut for the full kinematic range was performed using a Monte Carlo simulation.

For this purpose the Monte Carlo generator PHOJET [11] has been used, since it reproduces the measured transverse momentum spectra and charged particle multiplicities sufficiently well so that it can be employed for correcting experimental data.

In order to reject background from beam-gas interactions, the z coordinate of the vertex was restricted to $|z_{\rm Vtx}| < 35\,$cm. Further background rejection conditions were imposed, which require the timing of the event to match the bunch crossing time.

Imposing the cuts described in the previous sections, 23072 events met all criteria.

4 Cross Section Measurement

The aim is to measure the differential cross section $\mathrm{d}\sigma_{\gamma p\to Xp'}(ys, E_p')/\mathrm{d}z$. It can be determined using the relation

$$\frac{\mathrm{d}\sigma_{ep\to eXp'}(y,z)}{\mathrm{d}y\mathrm{d}z\mathrm{d}Q^2} = \mathcal{F}_{\gamma/e}(y,Q^2)\frac{\mathrm{d}\sigma^{\gamma p\to Xp'}(ys,z)}{\mathrm{d}z},$$

where $\mathcal{F}_{\gamma/e}(y,Q^2)$ is the photon flux in the Equivalent Photon Approximation [6].

The data have to be corrected for acceptances and efficiencies. Weights are introduced for the FPS trigger efficiency, the FPS track reconstruction efficiency, the track multiplicity dependent trigger efficiency, and the electron tagger acceptances. The latter includes a correction for cases where events are lost due to an energy deposition in the photon detector by a Bethe Heitler process occuring simultaneously with a photoproduction reaction, so called overlay events. Binwise correction factors are used to correct for track reconstruction efficiency in the H1 tracking chambers and to compensate the migration between proton energy bins and the limitation due to the finite FPS acceptance. The values for the migration corrections vary between 0.911 and 1.125, the acceptance corrections range from 0.269 to 0.903.

4.1 Background

The following sources of background were studied:

- Fake proton: A proton in the FPS can be faked by showers due to interactions of the proton beam with the beam pipe wall or residual gas. These particles do not originate from the nominal interaction point and fail to match a valid trajectory coming from the interaction point. The remaining background is negligibly small.
- Tracks in the central H1 detector produced by beam gas interactions: A handle on this kind of background is given by the z coordinate of the event vertex. The quantity $z_{\rm Vtx}$ is approximately Gaussian distributed in z around a mean value close to the nominal interaction point, while beam gas interactions show no correlation. The fraction of background events entering the data sample, where $|z_{\rm Vtx}| < 35\,$cm is required, can be estimated from the tails of the $z_{\rm Vtx}$ distribution and has been determined to vary between 2.2% (lowest y bin) and 3.4% (highest y bin). These numbers contribute to the systematic error.
- Bethe Heitler events $ep \to e'p'\gamma$: They are not a significant source of background since the acceptance for the photons is large and with the cut imposed on the maximum energy deposited in the photon detector these events are suppressed to a level of 0.3%.

4.2 Systematic errors

Three types of systematic errors are distinguished: errors common for events in the same y interval, errors related to the proton energy (or z) interval, and global errors.

Errors depending on y. The following sources contribute to this type of error: background from proton beam gas interactions in the central region of the H1 detector, errors on the acceptance of the electron taggers, errors on the selection efficiency for tracks in the H1 tracking chambers, and in case of ETAG33 an uncertainty of the positron energy measurement resulting in an imprecise determination of the number of events belonging to one of the two y bins. The individual contributions are listed in Table 1.

	ETAG44	ETAG33	
		$y^{\mathrm{ETAG}} < 0.5$	$y^{\mathrm{ETAG}} > 0.5$
proton beam bas background	2.2%	2.3%	3.4%
error on energy meas. (ETAG33)		0.8%	5.0%
central track selection	4.2%	3.3%	
ETAG acceptances	6%	5%	
total	7.6%	6.5%	8.5%

Table 1: *Systematic errors common for events in the same inelasticity bin.*

Errors depending on z. Uncertainties on the acceptance and migration corrections for each z bin are grouped together in Table 2.

For the acceptance correction, the biggest effect is related to the distribution of the proton's transverse momentum. The effect was evaluated using the PHOJET [11] and POMPYT [12] Monte Carlo generators. These two generators produce events with different p_T spectra of the scattered proton, while the description of the remaining hadronic final state is satisfactory in both cases. Because the transverse momentum distributions are not yet measured, the two programs have been used to get an estimate of the uncertainty for the correction.

The migration between z bins is greatly influenced by the stability of the FPS calibration procedure. To estimate this effect, the calibration was performed on subsamples of the Monte Carlo data set.

Global contributions. These are listed in Table 3 and are given by the uncertainty on the luminosity measurement, a value for FPS systematic errors such as alignment errors, uncertainty on the hodoscope efficiencies, and other effects not covered by the simulation. Additionally systematic errors on the vertex cut efficiency and positron beam related background are included.

z interval	migration	acceptance	total
$0.66 \ldots 0.71$	7.8%	11.8%	14.1%
$0.71 \ldots 0.76$	3.0%	3.1%	4.3%
$0.76 \ldots 0.80$	1.2%	1.3%	1.8%
$0.80 \ldots 0.85$	2.0%	1.6%	2.6%
$0.85 \ldots 0.90$	6.7%	5.2%	8.5%

Table 2: *Systematic errors common for all events in the same z bin. The error on the migration correction is the result of Monte Carlo studies investigating the influence of errors on the calibration constants. The error on the acceptance correction is estimated using two different Monte Carlo models.*

Source	
track reconstruction probability FPS	5%
Bethe Heitler background	0.3%
vertex cut	0.4%
luminosity	1.77%
normalization uncertainty	5.3%

Table 3: *Systematic errors common to all bins.*

4.3 Results

The cross section $\mathrm{d}\sigma_{\gamma p \to p' X}(W)/\mathrm{d}z$ for $W = 91,\ 187,$ and $231\,\mathrm{GeV}$ and five values of z for $0.66 \leq z \leq 0.90$ is shown in Figure 3. The errors shown are the sqare root of the quadratic sum of the systematic errors as described above and the statistical error taking into account the weights of the events. The total errors vary between 9.2% and 21.0%.

It is observed that in all z bins the measured cross-sections for different values of the γp centre-of-mass energy W agree with each other within the experimental errors. Furthermore the z dependence is only weak without a clear trend so that the present data may be represented by one average cross-section value of $7.7\,\mu$b per unit of z (the measured values ranging between 7.4 and 9.8) which corresponds to $\mathrm{d}\sigma_{\gamma p \to p' X}(W)/\mathrm{d}E'_p \sim 9.4\,\mathrm{nb}/\,\mathrm{GeV}$ for the kinematic range covered by this experiment. In particular the restriction in the transverse momentum of the final state proton to $p_T \leq 0.2\,\mathrm{GeV}$ should be kept in mind, which is equivalent to the statement that the measured cross-section represents only about 24% of the total semi-inclusive photoproduction cross-section if a slope of $b = 6.8\,\mathrm{GeV}^{-2}$ in $\mathrm{d}\sigma/\mathrm{d}p_T^2 \sim e^{-bp_T^2}$ is assumed as measured by the ZEUS collaboration [8].

The present data can be used to extend a measurement by the ZEUS collaboration [10] of the fraction of events with a leading proton with $0.60 < z < 0.97$ and $p_T^2 < 0.5\,\mathrm{GeV}^2$ compared to inclusive DIS events for $0.1\,\mathrm{GeV}^2 < Q^2 < 260\,\mathrm{GeV}^2$. The ZEUS experiment observes that this ratio is largely independent of the DIS scaling variables x and y over the Q^2 range covered by the experiment in [10]. At $Q^2 = 0$, the data have to be extrapolated to the kinematic range of the ZEUS experiment assuming $b = 6.8 \pm 0.8\,\mathrm{GeV}^{-2}$ and a flat z dependence in accordance with published data. It is found that at $Q^2 = 0$ this ratio is $r = 0.07 \pm 0.01$, within the errors compatible with the values measured at finite virtuality.

The observed z independence is in accord with the assumption of factorisation in a Regge description of the reaction.

From the fact that the cross-section is independent of z and W we infer that it is also independent of M_X, the mass of the hadronic final state apart from the leading proton. This observation is in contrast to diffractive processes, where a $1/M_X^2$ dependence is a good approximation to the data. The present measurement is reminiscent of data from semi-inclusive proton-proton scattering $p + p \rightarrow p + X$ at lower energy centre-of-mass energies squared $s < 3900\,\mathrm{GeV}^2$ [9], where a flattening of the cross-section $\mathrm{d}\sigma/\mathrm{d}M_X^2$ is observed for normalized masses above $M_X/\sqrt{s} \sim 0.2$, which is the same regime as covered by the present experiment.

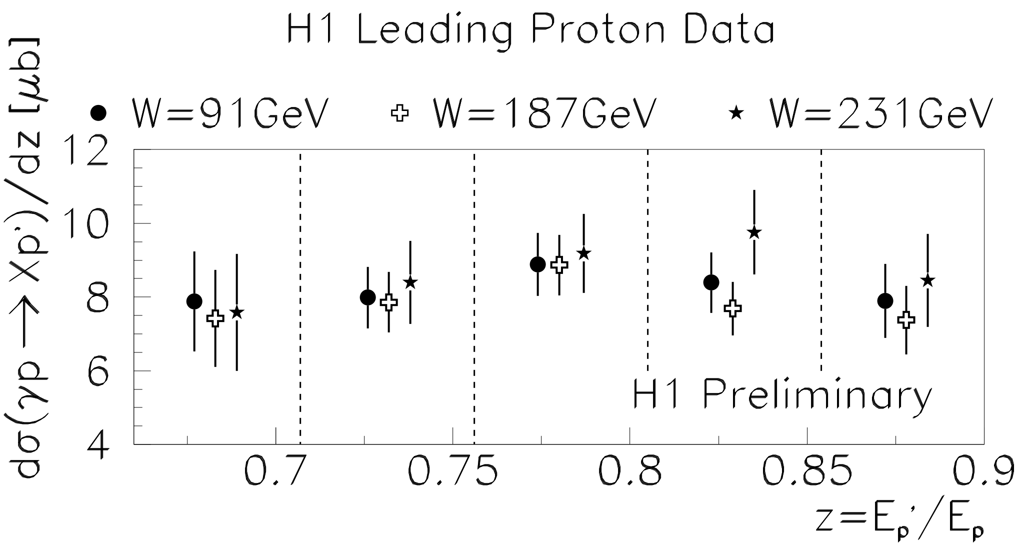

Figure 3: *The cross section* $d\sigma_{\gamma p \rightarrow p'X}/dz$ *as a function of* z *for three values of* W*. All data points in a box belong to the same* z *value (*$z = 0.682, 0.732, 0.780, 0.829, 0.878$*) and only for a better distinction they are drawn apart.*

5 Leading Proton Production in DIS and Photoproduction

5.1 Cross Section Measurement for Real and Virtual Photons

Applying Equation 1, inclusive deep inelastic scattering and inclusive photoproduction data from the reaction $\gamma^{(*)}p \rightarrow X$ have been combined in order to study the transition between the two kinematic regimes in [1]. In the present paper, the same investigation is performed for the process $\gamma^{(*)}p \rightarrow p'X$.

Data points on deep inelastic scattering with a leading proton observed in the FPS with the same set-up as used for the photoproduction investigation described in the previous chapters are published in [3]. Radiative corrections have been applied to the DIS data. They amount to not more than 6% for all bins in (x, Q^2).

The kinematic range covered by the DIS data sample is $0.707 \leq z \leq 0.902$, divided into four same-size intervals, $2\,\mathrm{GeV}^2 \leq Q^2 \leq 50\,\mathrm{GeV}^2$ in five bins, and $6 \cdot 10^{-5} \leq x \leq 6 \cdot 10^{-3}$ in four bins. A structure function $F_2^{LP(3)}$ was defined as:

$$\frac{\mathrm{d}^3\sigma}{\mathrm{d}x\mathrm{d}Q^2\mathrm{d}z} = \frac{4\pi\alpha^2}{xQ^4}\left(1 - y + \frac{y^2}{2[1 + R(x, Q^2, z)]}F_2^{LP(3)}(x, Q^2, z)\right),$$

where $R(x, Q^2, z)$ is the ratio of the longitudinal and the transverse DIS cross-sections with a leading proton. The impact of $R(x, Q^2, z)$ on the leading proton structure function $F_2^{LP(3)}(x, Q^2, z)$ is small. In the worst case a change of 9% is introduced when $R = \infty$ is assumed instead of $R = 0$. For the present analysis R is set to zero. This structure function is related to the leading proton photoproduction data as follows:

$$\frac{\mathrm{d}\sigma_{\gamma^{(*)}p \to p'X}(W)}{\mathrm{d}z} = \frac{4\pi^2\alpha}{Q^2}F_2^{LP(3)}(x, Q^2, z).$$

5.2 Model

In [1], the data have been contrasted with a model where the proton structure is assumed to consist of two components: F_2^{VDM} dominant at low values of the photon virtuality describing the contribution of vector mesons coupling to the virtual photon, and a partonic structure function F_2^{part}, governing the region $Q^2 > 1\,\mathrm{GeV}^2$ [13]. In [1], deep inelastic scattering data were fitted to the functional form

$$F_2(x, Q^2) = C_{VM}F_2^{VDM}(x, Q^2) + \frac{Q^2}{Q^2 + Q^2_{VM}}F_2^{H1QCD}(\bar{x}, Q^2 + Q^2_{VM}).$$

with $\bar{x} = (Q^2 + Q^2_{VM})/(W^2 + Q^2 + Q^2_{VM})$. The VDM part of the structure function is given by $F_2^{VDM}(x, Q^2) = Q^2/(4\pi)\sum_V(M_V^4\sigma_{Vp}(W))/(\gamma_V^2(Q^2 + M_V^2)^2)$, the sum running over the low mass vector mesons. The parameters γ_V and M_V represent the vector meson's coupling to the photon and its mass, respectively. The cross section for the Vp scattering is given by $\sigma_{Vp}(W)$. The contribution for F_2^{part} was taken from the structure function measurement. The fit parameter Q^2_{VM} was found to be $0.45\,\mathrm{GeV}^2$. The relative normalization C_{VM} of the vector meson term is not part of the model [13] but was introduced as a free parameter in order to match the photoproduction data. The fit resulted in $C_{VM} = 0.77$.

The model of [13] has not been developed to cover reactions with a leading proton, which according to the Feynman diagram of Figure 1 corresponds to a situation where the real or virtual photon interacts with a colourless constituent of the proton and not the proton itself. An argument, however, could be made that also the exchange object has a partonic content and the VDM part describes a vector meson-reggeon or pion scattering process so that an equivalent ansatz as in the inclusive case could be justified. Therefore, making use of the observation that also the deep inelastic semi-inclusive cross-section is nearly independent of W and z, two

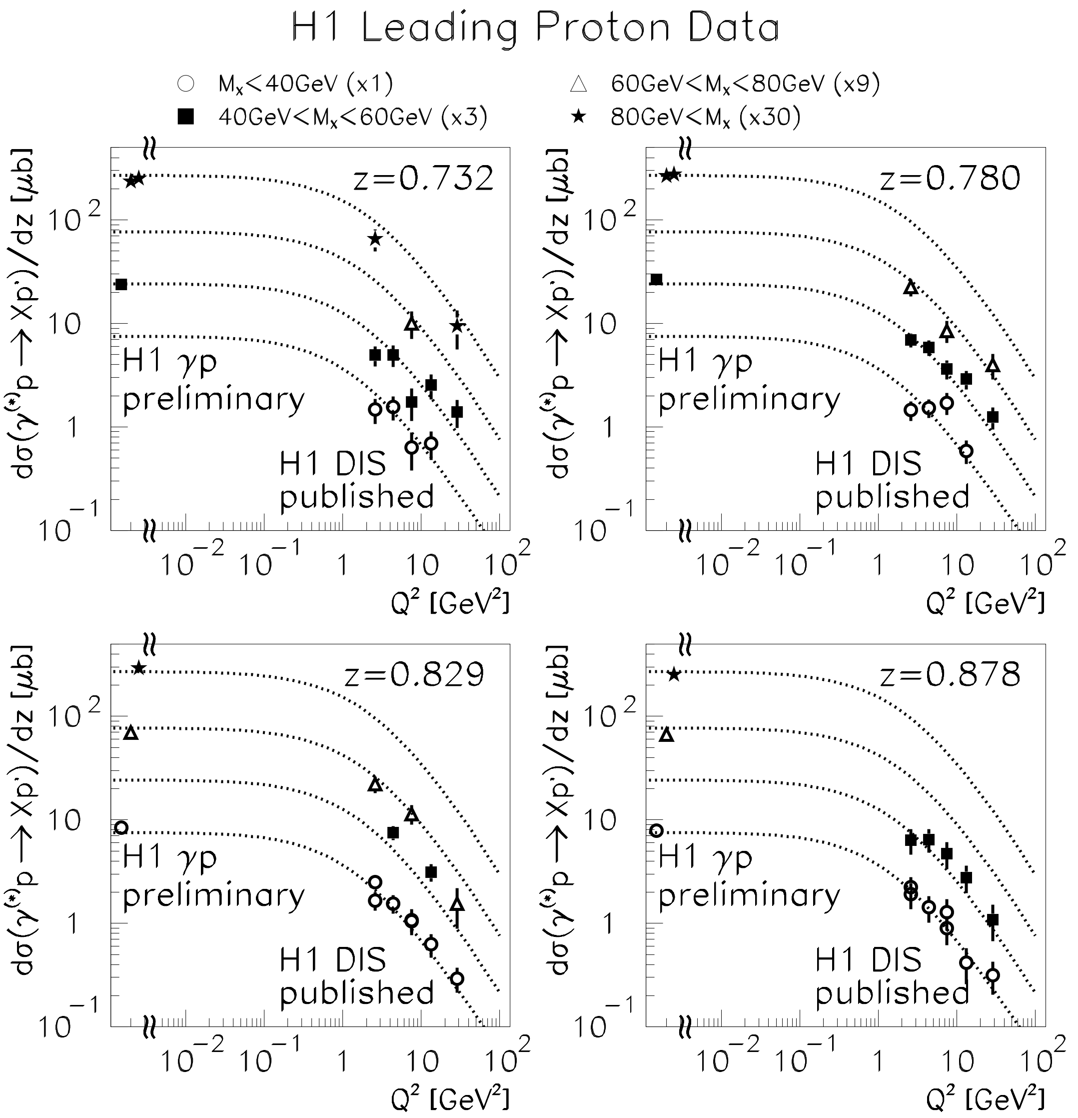

Figure 4: *The cross section $d\sigma_{\gamma^{(*)}p\to p'X}/dz$ for four bins of z and four bins of M_X as a function of Q^2.*

additional parameters are introduced: a common scale factor F including the flux factor for the emission of particles $\mathcal{R}$ by the proton and a compensation for the reduction in phase space due to the limited transverse momentum of the scattered protons, and a normalization factor C_{VM}^{LP} for the vector meson contribution. The variable comparable to x of the inclusive case is $\beta = x/(1-z)$ here. The function is modelled as follows:

$$\frac{F_2^{LP(3)}(x, Q^2, z)}{F} = \left(0.77 \cdot C_{VM}^{LP} F_2^{VDM}(\beta, Q^2) + \frac{Q^2}{Q^2 + 0.45} F_2^{H1QCD}(\bar{\beta}, Q^2 + 0.45)\right).$$

Since no data in the genuine transition region is available, the contributions to F_2^{LP} are fixed independently. The global factor F is determined by the DIS data alone, resulting in $F = 0.12$, independent of the z and M_X. With F fixed, a common fit is made to the semi-inclusive DIS and photoproduction data. In this fit the parameter C_{VM}^{LP} is determined by the the photoproduction data alone with negligible impact on F_2^{H1QCD}. The set of values obtained for C_{VM}^{LP} ranges from 0.13 to 0.30 with errors such that a averaging process is justified. A mean value of $C_{VM}^{LP} = 0.23 \pm 0.10$ is obtained.

It is thus observed that the VDM term is suppressed by a factor of 0.23 with respect to the inclusive case. This is significantly smaller than the factor of 0.65 between the total cross sections for pion proton and proton proton scattering, which one would expect to be applicable if cross-sections were related to the number of quarks involved in a particular reaction.

The fits are displayed in Figure 4 together with the DIS and photoproduction data points. Like in the case of inclusive reactions, a transition region is observed near $Q^2 \approx 1\,\mathrm{GeV}^2$, where the DIS cross-section turns over into a non-scaling regime and approaches the photoproduction value.

Unfortunately the semi-inclusive data are not precise enough and do not cover a sufficiently wide range in M_X to study the transition as a function of M_X in all Q^2 bins.

6 Summary

Photoproduction reactions with a final state proton of $p_T \leq 0.2\,\mathrm{GeV}$ observed in the H1 Forward Proton Spectrometer have been analysed in the kinematic range $0.66 \leq z \leq 0.90$ at γp centre-of-mass energies $W = 91$, 187 and $231\,\mathrm{GeV}$. The cross section $\mathrm{d}\sigma(W)/\mathrm{d}z$ was determined to be on the average $7.7\,\mu$b per unit of z. It is independent of z and W within the experimental errors.

The fraction of events with a leading proton extrapolated to the kinematic range $0.60 < z < 0.97$ and $p_T^2 < 0.5\,\mathrm{GeV}^2$ compared with the total γp cross section is 0.07 ± 0.01. This result is compatible with values measured by the ZEUS collaboration for $0.1\,\mathrm{GeV}^2 < Q^2 < 260\,\mathrm{GeV}^2$.

The combination of data from photoproduction and deep inelastic scattering with a final state proton observed in the FPS, $\gamma^{(*)}p \to p'X$, in the kinematic range $0.71 \leq z \leq 0.90$ shows that a qualitatively similar behaviour as observed when going from virtual to real photons in the inclusive reaction $\gamma^{(*)}p \to X$ is expected. A model where the contributions to the cross section are divided into a VDM and a partonic component shows a fair description of the data, provided the overall normalization and the relative normalization between the two components are adjusted accordingly. However, the relative size of the vector meson fraction w.r.t. the partonic contribution within the model is 23% of the value found for the inclusive reaction.

7 Acknowledgements

We are grateful to the HERA machine group whose outstanding efforts have made and continue to make this experiment possible. We thank the engineers and technicians for their work constructing and maintaining the H1 detector, our funding agencies for financial support, the DESY technical staff for continuous assistance, and the DESY directorate for the hospitality which they extend to the non-DESY members of the collaboration. The forward proton spectrometer was supported by the INTAS93-43 project and the NATO contract PST.CLG.975100.

References

[1] H1 Collab., C. Adloff *et al.*, Nucl. Phys. B 497 (1997) 3–30

[2] A. Donnachie, P.V. Landshoff, Phys. Lett. B 296 (1992) 227–232

[3] H1 Collaboration, C. Adloff *et al.*, Eur. Phys. J. C 6 (1999) 587-602

[4] H1 Collaboration, I. Abt *et al.*, Nucl. Instrum. Meth. A 386 (1997) 310–347

[5] P. Van Esch *et al.*, Nucl. Instrum. Meth. A 446 (2000) 409–425

[6] S. Frixione *et al.*, Phys. Lett. B 319 (1993) 339–345

[7] J.J. Sakurai, D. Schildknecht, Phys. Lett. B 40, Nr. 1 (1972) 121–126

[8] ZEUS preliminary in ”Proceedings of ICHEP98 Conference, Vancouver”, p. 924, World Scientific A. Astbury et al. ed.

[9] M.G. Albrow *et al.*, Nucl. Phys. B 108 (1967) 1–29

[10] A. Garfagnini for the ZEUS collaboration: ZEUS preliminary in ”Proceedings of EPS HEP Conference, Tampere, Finland”, in press

[11] R. Engel, ”PHOJET manual (Program version 1.05c, June 96)”, University of Siegen preprint 95-05 (1995) (revised Feb. 96)

[12] P. Bruni, A. Edin, G. Ingelman, ”POMPYT version 2.6 – A Monte Carlo Program to Simulate Diffractive Hard Scattering Processes”, unpublished program manual (1996), see `http://www3.tsl.uu.se/thep/pompyt`

[13] B. Badełek, J. Kwieciński, Phys. Lett. B 295 (1992) 263–268